Available online at www.sciencedirect.com
SCIENCE DIRECT®
Sensors and Actuators A 120 (2005) 383–389
SENSORS AND ACTUATORS A PHYSICAL
www.elsevier.com/locate/sna

UV-LIGA interferometer biosensor based on the SU-8 optical waveguide

B.Y. Shew [a,*], C.H. Kuo [b], Y.C. Huang [b], Y.H. Tsai [a]

[a] *Device Technology Group, National Synchrotron Radiation Research Center, Hsinchu 30077, Taiwan*
[b] *Department of Mechanical Engineering, National Chiao-Tung University, Hsinchu 30077, Taiwan*

Received 19 August 2004; received in revised form 24 December 2004; accepted 8 January 2005
Available online 3 February 2005

Abstract

SU-8 resist was used as a core/cladding waveguide material to fabricate a Mach–Zehnder interferometer (MZI) for biochemical sensing. The refractive index of the SU-8 resist was fine-tuned with a Δn of 0.004 for single-mode transmission. The UV lithography processes of the SU-8 resist were also optimized to pattern the high resolution (1 μm) and high aspect ratio ($A_R = 6$) Y-branch structure of the optical interferometer. Optical measurements reveal that the SU-8 MZI chip can efficiently transmit the NIR laser ($\lambda = 1310$ nm) with a total loss less than 6 dB. When one branch of the MZI is in contact with the analyte, the interfered intensity stabilizes after the soaking time exceeds 5 min. NaCl solution with a concentration of 10^{-9} g/l can be detected using the SU-8 MZI chip. In the future, the polymer MZI chip can be mass-produced by molding process (or the LIGA process). The low-cost, label-free, real-time and high-sensitivity MZI chip will benefit many applications related to biological, environmental and industrial detection.

Keywords: Optical waveguide; Interferometer; Biochemical sensor; SU-8 resist; LIGA process

1. Introduction

A biosensor is an analytical device that consists of a biological recognition element and a signal transducer, which together relate the concentration of an analyte to a measurable response. The bioactive component could be an enzyme, an antibody, a cell, a tissue slice, a receptor or nuclei acid. The transducer of a biosensor is employed to convert the biological-recognition step into a signal that can be coupled to a microprocessor for control and measurement [1,2]. Such devices are usually divided into four categories—electrochemical, optical, piezoelectric and calorimetric. Optical biosensors are the most popular because they provide the advantages of high sensitivity, fast response time, in situ monitoring and the absence of electrical interference [3,4]. Among them, the SPR (surface plasmon resonator) biosensor is the most popular optical biosensor at present [5,6]. The sensitivity of the SPR is as high as 10^{-8} g/l, however, the detecting peripherals of the SPR sensor are quite complex and limit its range of applications. Improving sensitivity is also an endless target because it relate to how early a disease is detected.

The optical interferometer is another high-sensitivity device, which can be used as a biosensor [7–9]. In a typical configuration of the Mach–Zehnder interferometer (MZI), the guiding light is divided into two branches by means of a Y-junction. If one branch is functionalized in a way that analytic molecules can be adsorbed specifically on it, then the guided light in this branch will be phase-shifted by affecting its effective refracting index. A second Y-junction recombines the two branches, which then interfere with each other. The MZI thus converts the bio-recognition dependency into an intensity modulation. Due to the combination of interferometric detection and relatively long interaction length, the sensitivity of the MZI sensor is reported more than one order

* Corresponding author. Tel.: +886 35780281; fax: +886 35783813.
E-mail address: yuan@nsrrc.org.tw (B.Y. Shew).

0924-4247/$ – see front matter © 2005 Elsevier B.V. All rights reserved.
doi:10.1016/j.sna.2005.01.004

higher than that of the SPR sensor. The label-free MZI method also provides a real-time measurement of the biochemical reaction such as kinetic examinations of the antigen–antibody reaction. Moreover, the peripheral of the MZI sensor can be rather simple because the MZI chip itself exhibits very high functionality.

Silicon oxynitride and silica are commonly used as the core and cladding materials, which are patterned into the waveguide structures by repeating deposition and plasma etching [8]. Accordingly, the process time is long and the fabrication cost is very high. In this work, an attempt is made using the SU-8 resist to fabricate an MZI device for bio/chemical sensing. SU-8 is a negative-tone, chemically amplified resist that has been extensively used in MEMS applications [10]. Since the epoxy-based SU-8 resist has good optical transparence [11], it is then used as the waveguide materials in various integrated optical systems [12,13]. However, most of them are fabricated for multimode transmission or straight single-mode waveguiding. In this work, single-mode transmission with Y-junction component is required for a high-sensitivity MZI sensor. The problems both in optical characteristics and micromachining of the SU-8 resist have to be overcome to meet the requirements for the MZI sensor. Once the SU-8 MZI device has yielded the expected performance, it can be mass-produced via polymer molding, or the so-called UV-LIGA process. The low-cost, high-sensitivity polymer MZI chip will benefit many applications in biological, environmental and industrial detection in the future.

2. MZI design

In an optical waveguide, the light is guided in the core by total reflection from the core/cladding interface. The mode number (N_m) inside the waveguide can be calculated to be [14]

$$N_m = \left(\frac{2\pi a}{\lambda}\right)^2 \frac{n_1^2 - n_2^2}{2} \quad (1)$$

where a is the core dimension; l the wavelength; n_1 and n_2 the refractive indices of the core and cladding. In order to achieve higher sensitivity of the MZI, a single-mode transmission is required. Accordingly, the core dimension (a) and the Δn ($n_1 - n_2$) must be small, which then raise difficulties in micromachining and material technology. Meanwhile, the optical phase change ($\Delta\phi$) resulted from a change in the refractive index at the waveguide surface can be expressed as [9]:

$$\Delta\phi = L\frac{2\pi}{\lambda}\left(\frac{\partial N}{\partial n_{c,eff}}\right)\Delta n_{c,eff} \quad (2)$$

where L is the interaction length; N the effective refractive index of the propagating mode; $\Delta n_{c,eff}$ the change in the refractive index of the cover due to surface reactions. After

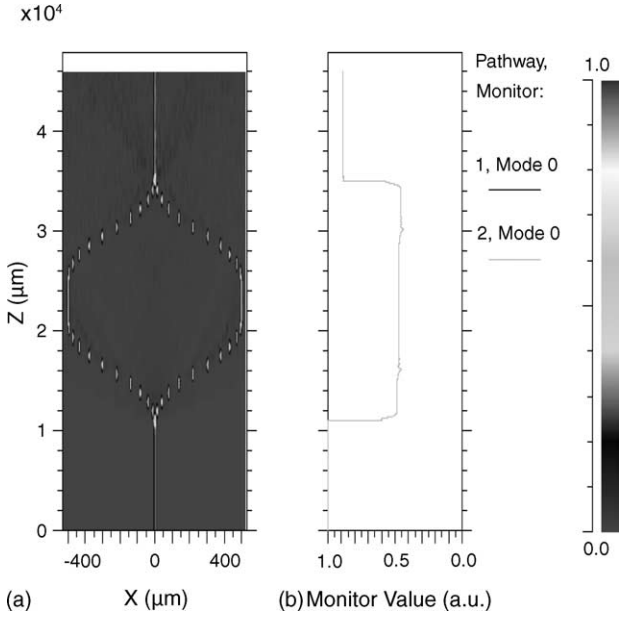

Fig. 1. Simulated fields (a) and transmission efficiency (b) in the MZI chip. The simulation was done based on the optical parameters designed in this work.

balancing all the parameters, including the micromachining capability, the optical property of the polymer materials, the optical coupling efficiency and the detection sensitivity, an MZI device is designed as follows: an NIR laser with a wavelength of 1310 nm is used as the guiding light. The thickness and the width of the core are 6 μm; the Y-branch tip is 1 μm wide; the Δn between the core and cladding is 0.004; and the interaction length of the MZI is 1 cm. An optical simulation tool of BeamPROP (Rsoft Design Group, Inc., USA) was used to simulate the propagation and transmission efficiency in the MZI chip. As presented in Fig. 1, the designed MZI chip can guide the light efficiently with a theoretical transmission efficiency of only around 0.4 dB. This MZI chip will be realized in the subsequent steps.

3. Modification of refractive index

The refractive index of the waveguide materials must be carefully controlled to provide single-mode, high-efficiency light transmission. In particular, the Δn of the core/cladding materials is only 0.004 in this MZI design, the modulation and control of the refractive index is very critical. In this work, the refractive index of the SU-8 resist was accurately measured using a prism coupler (Model 2010, Metricon, USA) with a resolution of 0.0005 [15]. A quartz prism was used in the measurement. As shown in Fig. 2, the refractive index of the as-lithographed SU-8 resist is 1.574. An attempt was made to use UV radiation to alter the refractive index of the SU-8 resist by the UV bleaching effect; however, no notable change in refractive index was observed even the UV exposure time

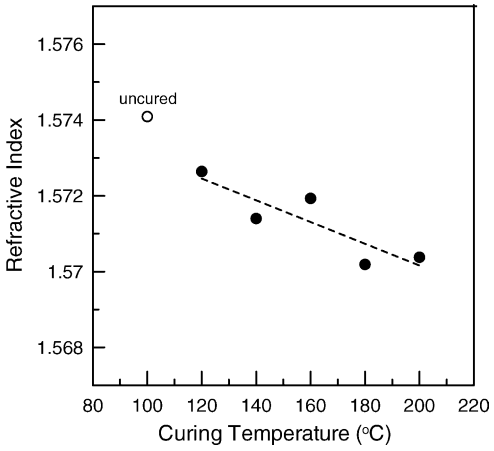

Fig. 2. Refractive index of the SU-8 resist after curing for 3 min at various temperatures.

was extended. In contrast, the refractive index of the resist declines consistently as the curing (hard-baking) temperature increases (Fig. 2). The decreases in refractive index probably because the molecular weight (M) of the resist increase after thermal treatment, as indicated by Lorentz–Lorentz equation [16]:

$$\frac{n^2-1}{n^2+2} = \frac{N}{3M\varepsilon}\rho\beta \tag{3}$$

where N is the Avogadro's number, ρ the density, ε the permittivity, and β the mean polarizability of the molecules, which is almost constant upon polymerization [16].

Fig. 2 also indicates that the refractive index of the resist is about 1.570 after curing at 200 °C for 3 min. The Δn of the uncured/cured resist is approximately 0.004, meeting the specification of the designed MZI chip. Optical measurements (Fig. 3) also reveal that the refractive indices remained constant when the resists were cured at 200 °C for various times, suggesting that the modification process is rather stable. Therefore, the uncured/cured SU-8 resist were employed directly as the core/cladding materials herein.

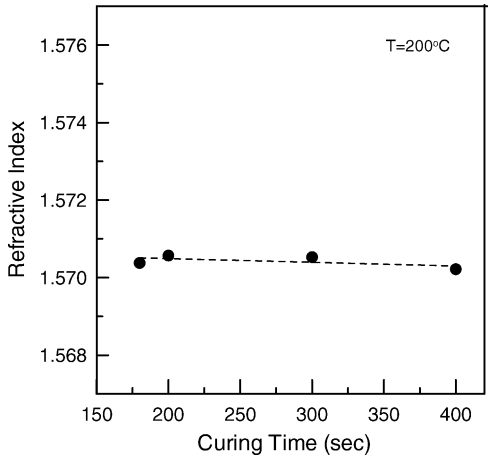

Fig. 3. Refractive index of the SU-8 resist after curing at 200 °C for various times.

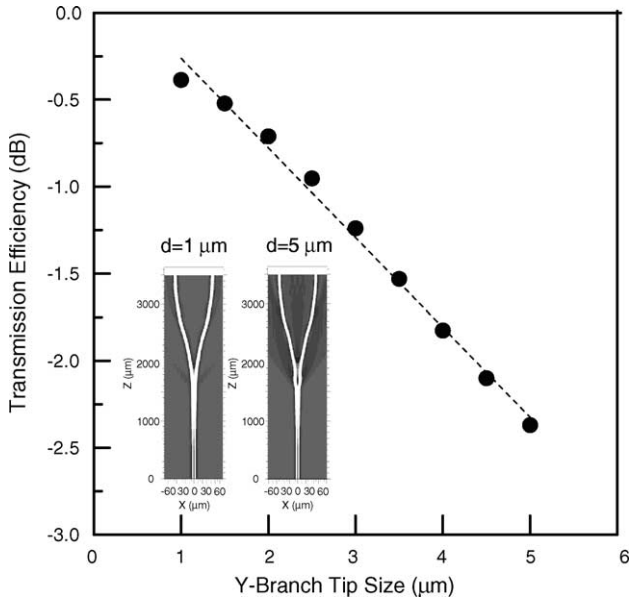

Fig. 4. Transmission efficiency of the MZI chip vs. the tip size of the Y-branch. The simulated fields at the Y-junction with a tip size of 1 μm and 5 μm are also presented in the figure.

4. High-resolution UV lithography

In an MZI device, the light is split and recombined by the Y-branch structure. The major constraint when designing Y-junction is the transmission losses due to the minimum width of the gap between the two branching waveguides (Y-branch tip) limited by photolithography or etching processes [17]. As illustrated in Fig. 4, the simulated transmission efficiency through the MZI chip decreases consistently as the tip size increases; the signal/noise ratio, or the detection sensitivity will be degraded in consequence.

Fig. 5(a) presents the top view of the SU-8 Y-branch structure following conventional lithographic processes. The patterned tip width is around 3.6 μm, which is much larger than the designed value (1 μm) of the MZI device. The enlarged tip results mainly from the Fresnel diffraction in contact printing process, and the maximum diffraction error (MDE) can be expressed as [18]:

$$\mathrm{MDE} = \frac{(1+1.5\bar{g})\sqrt{\lambda T}}{2}\left(\sqrt[4]{\exp(b)\left(1+\frac{a}{4}\right)}-1\right) \tag{4}$$

where T is the resist thickness; $\bar{g} = g/T$ and g the gap between mask and resist, $a = AT$ and A the kinetic absorption coefficient of the resist, which is related to the time-dependent photochemical reaction, $b = BT$ and B the natural absorption coefficient of the resist matrix. Since the resist material and thickness are given in this work, the resist absorptance to the exposure source has to be minimized for achieving higher resolution.

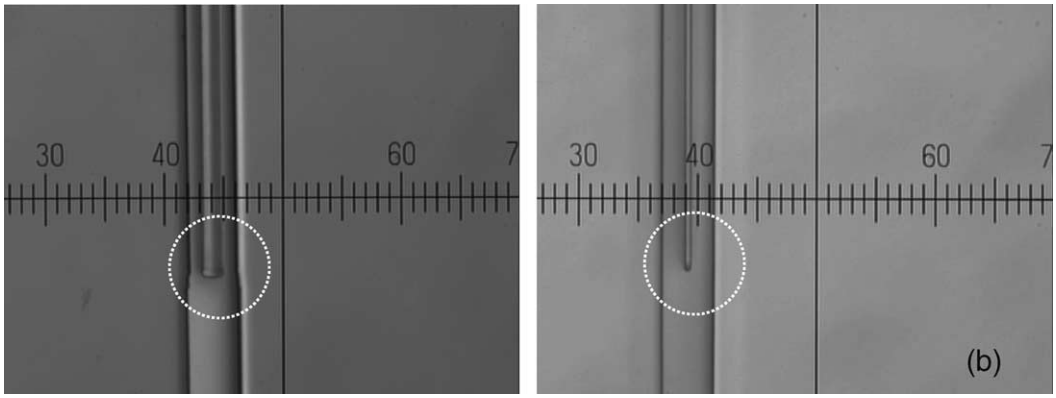

Fig. 5. Optical photographs of the lithographed SU-8 Y-branch tip: (a) before and (b) after removing the high-energy irradiation in the exposure light source.

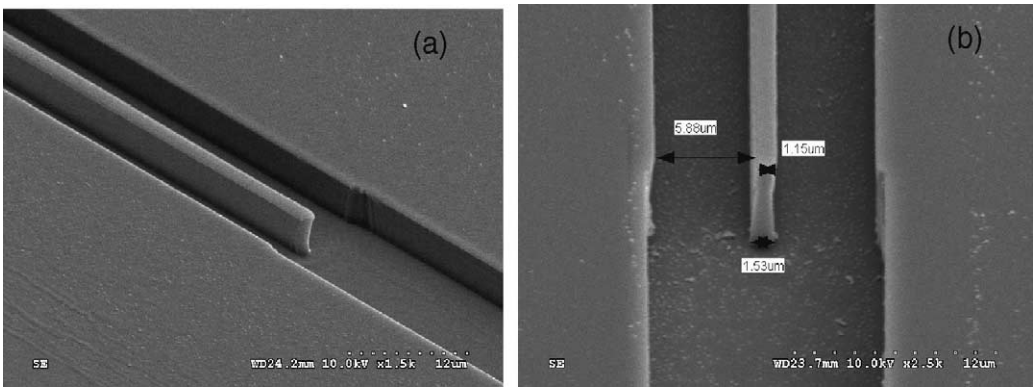

Fig. 6. SEM photographs of the lithographed SU-8 Y-branch tip. The thickness of the waveguide is around 6 μm.

SU-8 resist is conventionally patterned by i-line ($\lambda = 365$ nm) irradiation [10]. The resist is very transparent to near UV (365–440 nm); however, its absorptance increases markedly as the wavelength lower than 365 nm. In a conventional Hg-lamp, the irradiating spectrum includes middle and deep UV other than near UV. The high-energy irradiation, which is strongly absorbed by the SU-8 resist, will degrade the lithographic resolution of the SU-8 resist according to Eq. (3). In this study, two dichromic mirrors were employed to remove the high-energy photons ($\lambda < 365$ nm) from the Hg-lamp source for achieving higher lithographic resolution. As illustrated in Fig. 5(b), the patterned tip size of the Y-junction is about 1.2 μm—much close to the target dimensions. SEM photography (Fig. 6) also reveals that the micromachining quality of the SU-8 Y-branch structure is rather good. The deviation of the width of the waveguide is less than 0.5 μm, which will lead to a better transmission efficiency of the guiding light.

5. MZI chip fabrication

The MZI chip was fabricated as illustrated in Fig. 7, according to the resist processes explicated above. First, a 6 μm thick SU-8 resist was spin-coated and floor-exposed on the silicon wafer substrate. A second layer of SU-8 resist with the same thickness was UV lithographed to fabricate the waveguide structure with high resolution and high aspect ratio. After that, the cladding resist was cured at 200 °C for 3 min,

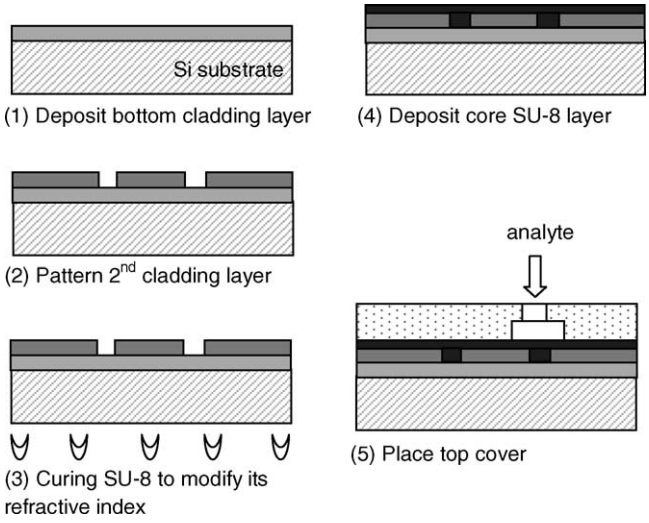

Fig. 7. Fabrication processes of the SU-8 MZI chip.

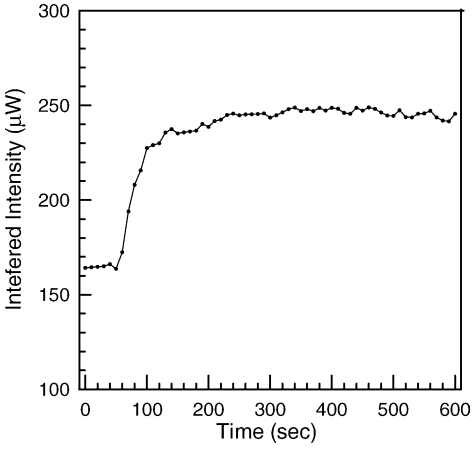

Fig. 8. Interfered intensity against soaking time when one branch of the MZI is in contact with the NaCl solution (10^{-6} g/ml).

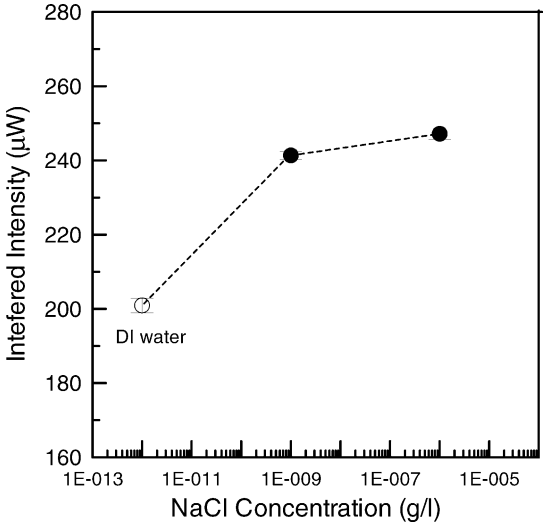

Fig. 9. Interfered intensity of the MZI chip when one branch is soaked in the NaCl solution at various concentrations.

reducing its refractive index to about 1.570. A third layer of SU-8 resist was then spin-coated, and floor-exposed as the core layer of the waveguide. The spin speed was carefully controlled to minimize the thickness of the rib of the core layer. Except for the standard resist processes, no extra thermal treatment was applied to the core SU-8 layer, so its refractive index will be around 1.574. Finally, a PDMS sheet was applied on the top of the rib waveguide as a top cladding layer. The PDMS cover was also machined to fabricate a fluidic channel for transporting analyte in the subsequent experiment.

6. Optical measurement

Once the MZI chip was fabricated, a non-polarized NIR laser with a wavelength of 1310 nm (1 mW) was end-fire coupled into the MZI chip through a single-mode optical fiber. Using an IR CCD, the guiding light at the two branches and at the exit of the MZI can be easily observed. Optical measurements show that the total optical loss is about 6 dB, which is higher than the theoretical loss as discussed previously. The optical loss is composed of intrinsic and extrinsic loss. The intrinsic loss is estimated around 4 dB since the absorption loss of the SU-8 is about 1.36 dB/cm [11] and the waveguide length is about 3 cm. The extrinsic loss, which mainly resulted from optical coupling and waveguide imperfection, probably contribute the rest of the optical loss (∼2 dB). However, the transmission efficiency of the SU-8 MZI chip is good enough for subsequent sensor applications.

In this investigation, NaCl solutions with various concentrations were employed to test the performance of the MZI sensor. If the SU-8 MZI chip works well, it should detect a tiny change in the refractive index of the NaCl solution with any of the various concentrations. The laser was end-fire coupled into and out of the MZI chip. The interfered intensity was then measured using a photodiode and recorded by a computer. Fig. 8 shows a typical curve of interfered intensity versus soaking time when one branch of the MZI is in contact with a NaCl solution (10^{-6} g/ml). In the first 60 s, the intensity remains unchanged; perhaps, the solution does not wet the waveguide surface. Thereafter, the intensity elevates suddenly and saturates at about 250 μW when the soaking time exceeds 300 s. Although the water absorptance of the epoxy-based SU-8 resist is rather low, it might result in a background signal in the MZI sensor. We will try to measure the contribution from the swelling effect. However, the background signal will be cancelled in the differential measurement (such as MZI sensor) if the swelling is uniform and stable.

Fig. 9 presents the interfered intensity of the MZI chip when one branch is soaked in NaCl solutions of different concentrations. The data were obtained by averaging the output intensity over a range of soaking times from 300 to 480 s. The standard deviation of the measurement is also plotted in the figure. As indicated in Fig. 9, the output intensity increases with the NaCl concentration (or refractive index), and a very low NaCl concentration of 10^{-9} g/l can be detected using the SU-8 MZI chip. In particular, a gap exists between the interfered intensity of the DI water and the NaCl solution, suggesting the potential for chasing higher sensitivity with the MZI device.

Since the SU-8 MZI device performs well, some future work will be done to yield the advantages of the polymer MZI sensor. The first task is to mass-produce the MZI chip by the UV LIGA process. In fact, a Ni mold has been replicated by electroforming from the SU-8 master. Preliminary results (Fig. 10) also show that the fine Y-branch structure can be fabricated by micro hot embossing. The resolution and dimensions of the molded waveguide structure meet the specification of the design but the surface quality must be further improved. Additionally, the bio-molecular probe will be immobilized on the surface of the polymer waveguide using AAc (acrylic acid) as the linking layer [19]. The grating

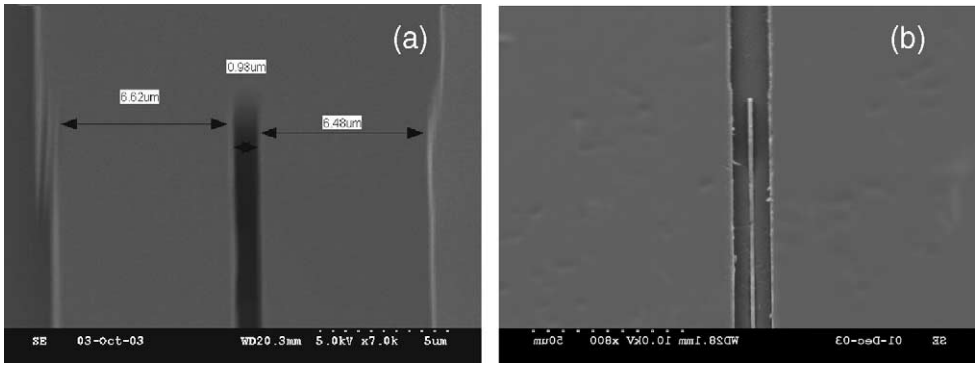

Fig. 10. SEM photographs of the (a) electroformed and (b) hot-embossed Y-branch microstructure.

or prism coupling will also be used to improve the coupling efficiency of the MZI sensor.

7. Summaries

The negative-tone, epoxy-based SU-8 resist was used to fabricate an MZI device for biochemical sensing. In order to achieve higher detection sensitivity, a single-mode transmission of the guiding light in the MZI chip is required. In consequence, the waveguide dimension and the differential of the core/cladding materials (Δn) must be small, which then raise difficulty in micromachining and material technology. In this study, the refractive index of the SU-8 resist was stably controlled with a Δn of 0.004 so that the uncured/cured resist could be used directly as the core/cladding layer of the optical waveguide. The lithography processes were also optimized to pattern the Y-branch structure with high resolution (1 μm) and high aspect ratio ($A_R = 6$). Especially, two dichromic mirrors were employed to remove the high-energy irradiation ($\lambda < 365$ nm) from the Hg-lamp source for reducing the diffraction error and then achieving higher lithographic resolution. Optical measurement results show that the SU-8 MZI chip can efficiently transmit the NIR laser ($\lambda = 1310$ nm). When one branch of the MZI is in contact with the analyte, the interfered intensity stabilizes when the soaking time exceeds 5 min; and a dilute NaCl solution with a concentration of 10^{-9} g/l can be detected using the SU-8 MZI chip. In the future, the bio-molecular probes will be immobilized on the surface of the polymer waveguide with an AAc (acrylic acid) linking layer. Furthermore, grating or prism coupling will be used to improve the coupling efficiency of the MZI sensor. A low-cost, label-free, real-time and high-sensitivity polymer MZI biosensor could be highly expected after this exploration.

Acknowledgement

The authors would like to thank the Union Chemical Laboratory and Opto-Electronics and Systems Laboratory of Industrial Technology Research Institute at Taiwan for their technical supporting on optical measurement of the materials and the devices.

References

[1] B.R. Eggins, Biosensors: An Introduction, Wiley, New York, 1996, pp. 1–117.
[2] S.S. Iqbal, M.W. Mayo, J.G. Bruno, B.V. Bronk, C.A. Batt, J.P. Chambers, A review of molecular recognition technologies for detection of biological threat agents, Biosens. Bioelectron. 15 (2000) 549–578.
[3] M. Mehrvar, C. Bis, J.M. Scharer, M. Moo-young, J.H. Luong, Fiber-optic biosensors—trends and advances, Anal. Sci. 16 (2000) 677–692.
[4] G. Boisde, A. Harmer, Chemical and Biochemical Sensing with Optical Fibers and Waveguides, Artech House, Boston, 1996.
[5] J. Homola, S.S. Yee, G. Gauglitz, Surface plasmon resonance sensors: review, Sens. Actuators B 54 (1999) 3–15.
[6] B. Liedberg, C. Nylander, I. Lundstro¨m, Biosensing with surface plasmon resonance—how it all started, Biosens. Bioelectron. 10 (1995) 1–9.
[7] S. Busse, M. DePaoli, G. Wenz, S. Mittler, An integrated optical Mach–Zehnder interferometer functionalized by β-cyclodextrin to monitor binding reactions, Sens. Actuators B 80 (2001) 116–124.
[8] F. Brosinger, H. Freimuth, M. Lacher, W. Ehrfeld, E. Gedig, A. Katerkamp, F. Spener, K. Cammann, A label-free affinity sensor with compensation of unspecific protein interaction by a highly sensitive integrated optical Mach–Zehnder interferometer on silicon, Sens. Actuators B 44 (1997) 350–355.
[9] R.G. Heideman, R.P.H. Kooyman, J. Greve, Performance of a highly sensitive optical waveguide Mach–Zehnder interferometer immunosensor, Sens. Actuators B 10 (1993) 209–217.
[10] L.K. LaBianca, S. Rishton, S. Zohlgharnain, Micromachining applications for a high resolution ultra-thick photoresist, J. Vac. Sci. Technol. B 13 (1995) 3012–3016.
[11] B. Bêche, N. Pelletier, E. Gaviot, J. Zyss, Single-mode TE_{00}-TM_{00} optical waveguides on SU-8 polymer, Opt. Commun. 230 (2004) 91–94.
[12] S. Balslev, B. Bilenberg, O. Geschke, A.M. Jorgensen, A. Kristensen, J.P. Kutter, K.B. Mogensen, D. Snakenborg, Fully integrated optical systems for lab-on-chip applications, in: Proceedings of the Conference, MEMS 2004, Maastricht, 2004, pp. 89–92.

[13] G.-B. Lee, C.-H. Lin, G.-L. Chang, Micro flow cytometers with buried SU-8/SOG optical waveguides, Sens. Actuators A 103 (2003) 165–170.
[14] J.P. Powers, An Introduction to Fiber Optic Systems, Aksen Associates Inc., Boston, 1993, pp. 17–24.
[15] T. Sharda, T. Soga, T. Jimbo, Optical properties of nanocrystalline diamond films by prism coupling, J. Appl. Phys. 93 (2003) 101–105.
[16] A. Cusano, G. Breglio, M. Giordano, A. Calabr'o, A. Cutolo, L. Nicolais, Optoelectronic characterization of the curing process of thermoset-based composites, J. Opt. A 3 (2001) 126–130.
[17] J. Gamet, G. Pandraud, Ultralow-loss 1×8 splitter based on field matching Y junction, IEEE Photon. Technol. Lett. 16 (2004) 2060–2062.
[18] Y. Cheng, C.Y. Lin, D.H. Wei, B. Loechel, G. Gruetzner, Wall profile of thick photoresist generated via contact printing, IEEE J. MEMS 8 (1999) 18–26.
[19] Z. Cheng, S.-H. Teoh, Surface modification of ultra thin poly (e-caprolactone) films using acrylic acid and collagen, Biomaterials 25 (2004) 1991–2001.

Biographies

B.Y. Shew received his BS in mechanical engineering (1989), and PhD in material science (1996) from the National Cheng-Kung University at Taiwan. He is at present the leader of Device Technology Group at National Synchrotron Radiation Research Center (NSRRC). His primary research area lies in LIGA technology, polymer micro optics, optical biosensors and photonic crystal device.

C.H. Kuo is a PhD candidate in the Department of Mechanical Engineering at National Chiao-Tung University.

Y.C. Huang is a graduate student in the Department of Mechanical Engineering at National Chiao-Tung University.

Y.H. Tsai received his MS in Department of Applied Chemistry at National Chiao-Tung University. He is currently an assistant researcher in device technology group at NSRRC.